First in Class Dual Non-ATP Competitive Glycogen Synthase Kinase 3β / Histone Deacetylase Inhibitors as a Potential Therapeutic to Treat Alzheimer's Disease

Alan Santini,[1] Elisa Tassinari,[1] Eleonora Poeta,[2] Manuela Loi,[3] Elisabetta Ciani,[3] Stefania Trazzi,[3] Rebecca Piccarducci,[4] Simona Daniele,[4] Claudia Martini,[4] Barbara Pagliarani,[1] Andrea Tarozzi,[1] Matteo Bersani,[5] Francesca Spyrakis,[5] Daniela Danková,[6] Christian A. Olsen,[6] Roberto Soldati,[1] Vincenzo Tumiatti,[1] Serena Montanari,[1] Angela De Simone,[5*] and Andrea Milelli[1*]

1 Department for Life Quality Studies, Alma Mater Studiorum-University of Bologna, Corso d'Augusto 237, 47921 Rimini, Italy

2 Department of Pharmacy and Biotechnology, Alma Mater Studiorum-University of Bologna, Via Francesco Selmi 3, 40126 Bologna, Italy

3 Department of Biomedical and Neuromotor Science, Alma Mater Studiorum-University of Bologna, Piazza di Porta S. Donato, 2, 40126 Bologna, Italy

4 Department of Pharmacy, University of Pisa, Via Bonanno Pisano, 6, 56126 Pisa, Italy

5 Department of Drug Science and Technology, University of Turin, Via Pietro Giuria 9, 10125 Turin, Italy

6 Center for Biopharmaceuticals & Department of Drug Design and Pharmacology, Faculty of Health and Medical Sciences, University of Copenhagen, Jagtvej 160, DK-2100, Copenhagen, Denmark

Corresponding Authors:
Angela De Simone, angela.desimone@unito.it
Andrea Milelli, andrea.milelli3@unibo.it

Table of contents

1. Table SI1. Effects of compounds **1-8**, tideglusib, vorinostat and nexturastat A, on GSK-3β, HDAC2, and HDAC6 activity.

2. Figure SI1. Protein surface and electrostatic potential map comparison between HDAC2 and HDAC6.

3. Figure SI2. HDAC2 and HDAC6 Molecular Interaction Field (MIF) pocket analysis.

4. Figure SI3. Contact map of compound **5** in HDAC2 and HDAC6.

5. Figure SI4. Solvent Accessible Surface Area (SASA) analysis of compound **5** in HDAC2 and HDAC6.

6. Figure SI5. Protein RMSD analysis of compound **5** in HDAC2 and HDAC6.

7. Figure SI6. Donor-acceptor pairs in HDAC2 and HDAC6 complexes with compound **5**.

8. Figure SI7. Cell viability in SH-SY5Y cells.

9. Figure SI8. Effect of treatment with Nexturastat A and Tideglusib on GSK-3β phosphorylation, and histone H3 alpha tubulin acetylation in SH-SY5Y cells.

10. Figure SI9. Immunomodulatory effects of Vorinostat, Nexturastat A, and Tideglusib on murine N9 cells

11. Table SI2. Assessment of compound **4** and parent compounds tideglusib and vorinostat with respect to some Molecular−Structural and Physicochemical properties.

12. Copies of ^{1}H- and ^{13}C-NMR spectra.

13. Table SI3. List of antibodies used.

1. Table SI1. Effects of compounds **1-8**, tideglusib, vorinostat and nexturastat A, on GSK-3β, HDAC2, and HDAC6 activity.

Compounds	% inhibition at 1 μM[a]		
	GSK-3β	HDAC2	HDAC6
1	44.78±22.43	36.24±13.40	36.99±5.59
2	47.31±4.57	21.95±2.43	37.23±2.51
3	54.64±6.07	55.93±5.02	78.43±0.74
4	95.33±0.61	88.43±0.49	89.39±0.82
5	87.81±2.90	86.65±2.80	87.68±0.23
6	91.93±3.02	85.70±3.87	88.36±0.29
7	35.65±3.96	63.07±2.16	44.84±3.08
8	94.45±0.73	88.47±1.25	86.80±0.40
Tideglusib	n.d.[b]	63.68±5.00	64.34±2.07
Vorinostat	n.a.[c]	t.i.[d]	t.i. [d]
Nexturastat A	37.60%	n.d.[b]	n.d.[b]

[a.] % of activity inhibition at 1 μM of compounds are reported as a mean value of at least three determinations; [b.] not determined; [c.] not active up to 50 μM; [d.] t.i.: total inhibition.

2.

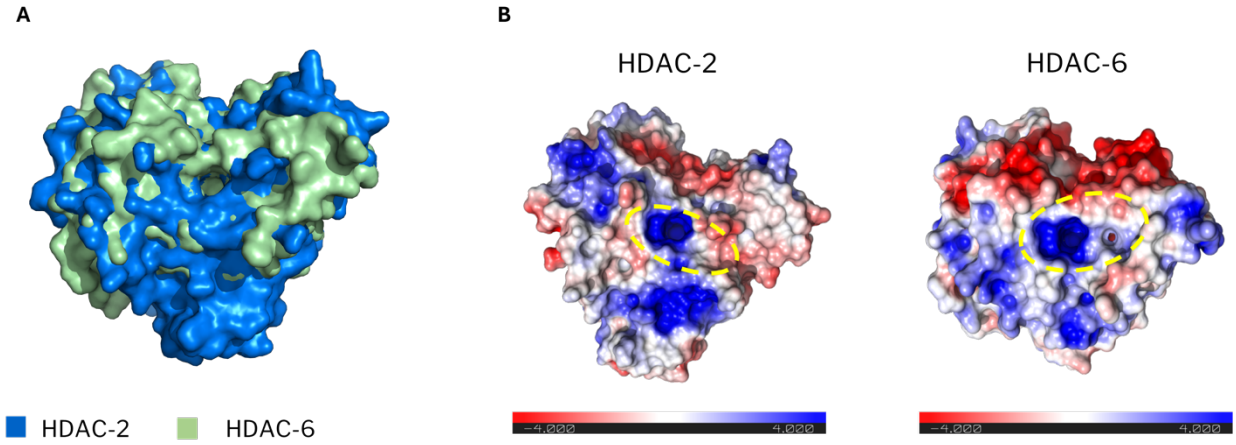

Figure SI1. Protein surface and electrostatic potential map comparison between HDAC2 and HDAC6. HDAC2 structure in complex with SAHA (PDB ID: 4LXZ) and HDAC6 structure in complex with TSA (PDB ID: 5EDU).

3.

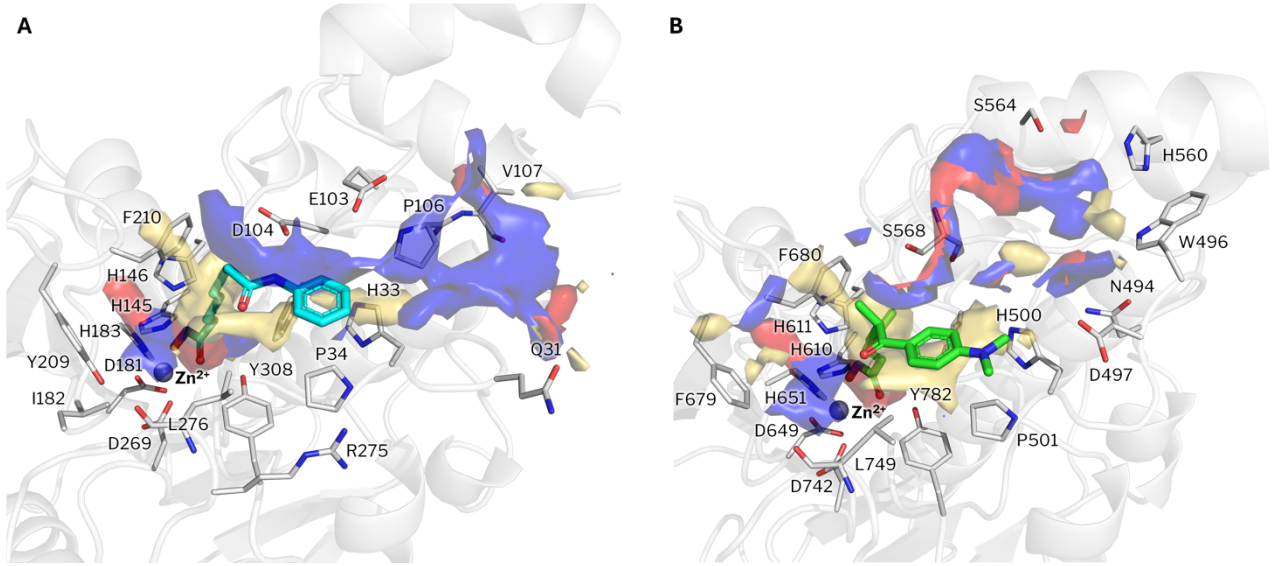

Figure SI2. HDAC2 and HDAC6 Molecular Interaction Field (MIF) pocket analysis. A) HDAC2 in complex with SAHA (PDB ID: 4LXZ); B) HDAC6 in complex with TSA (PDB ID: 5EDU). Red and blue contours identify respectively regions in which interactions with protein H-bond donors and acceptors are favorable. Potential protein hydrophobic interaction regions are highlighted

by yellow contours.

4.

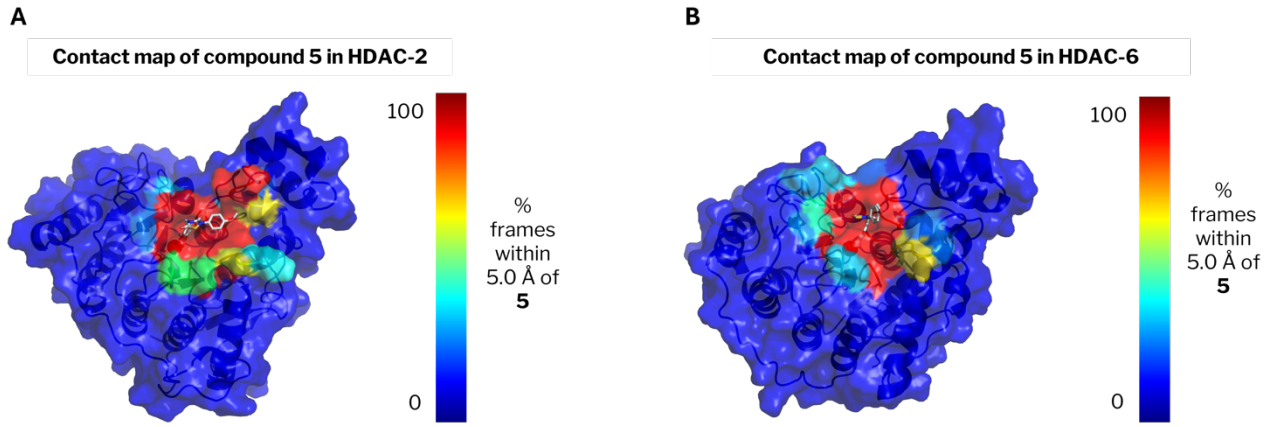

Figure SI3. Contact map of compound **5** in HDAC2 and HDAC6. Percentage of MD frames for each residue in which the center of mass is located within 5.0 A of the ligand.

5.

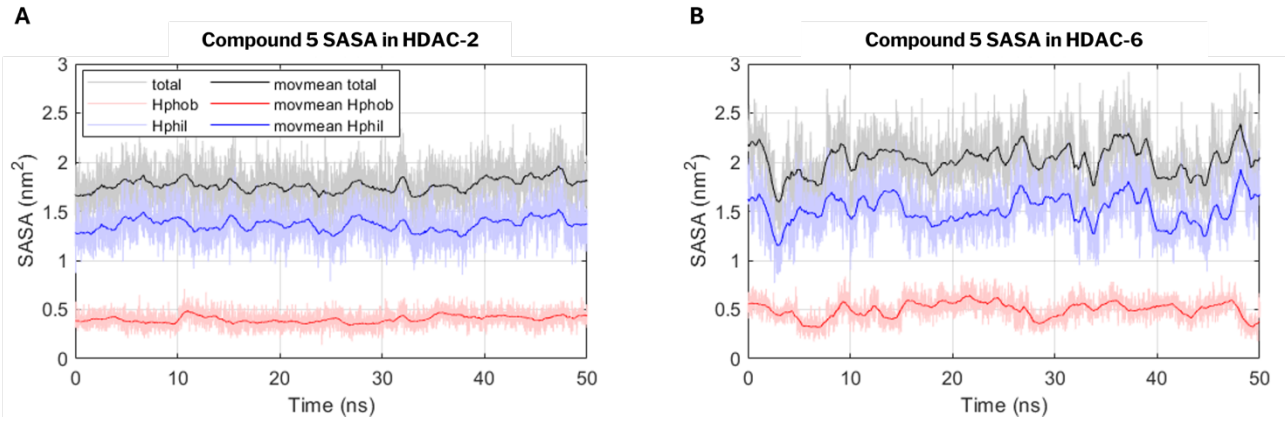

Figure SI4. Solvent Accessible Surface Area (SASA) analysis of compound 5 in HDAC2 and HDAC6. SASA hydrophobic, hydrophilic and total values along the 50ns MD simulation.

6.

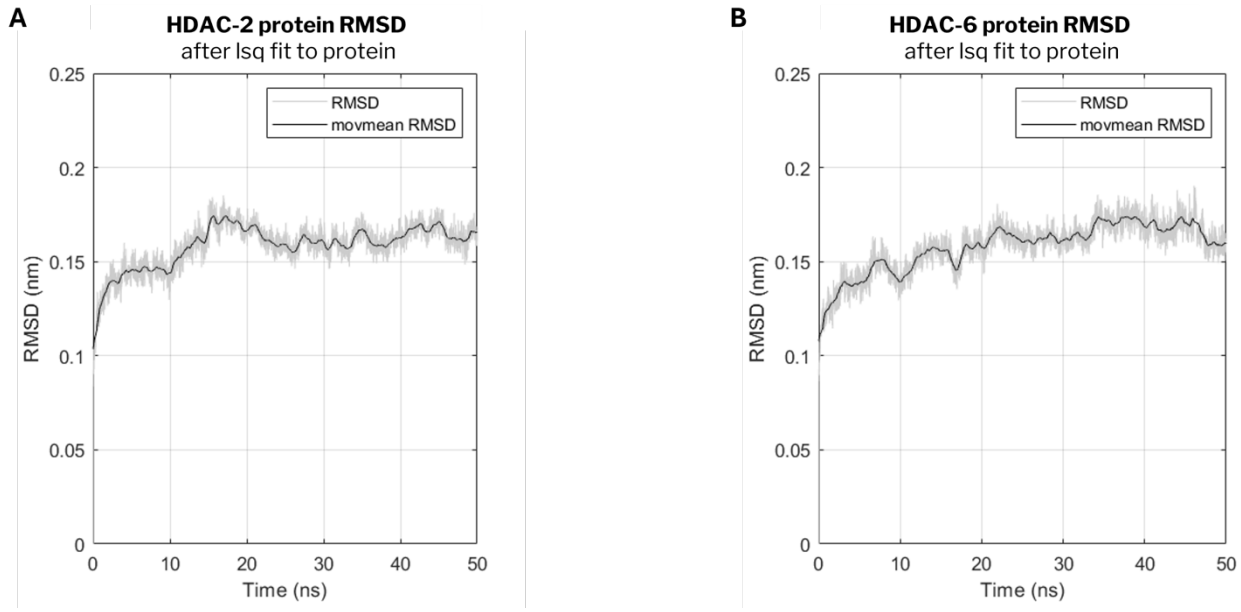

Figure SI5. Protein RMSD analysis of compound **5** in HDAC2 and HDAC6. RMSD values of the protein backbone along the 50ns MD simulation

7.

Donor-acceptor	H-bond occupancy (%)
308TYR(HH) - **5**(O1)	98.9
145HIP(HE2) - **5**(O2)	68.5
5(H5) - 146HID(NE2)	52.1

Donor-acceptor	H-bond occupancy (%)
610HIP(HE2) - **5**(O1)	82.1
782TYR(HH) – **5**(O2)	81.5
5(H5) - 611HID(NE2)	40.6
568SER(HG) - **5**(O3)	9.6

Figure SI6. Donor-acceptor pairs in HDAC2 and HDAC6 complexes with compound **5**. Pairs identified along the 50ns MD simulation in which the percentage of frames satisfying H-bond distance and angle criteria were higher than 5%.

8.

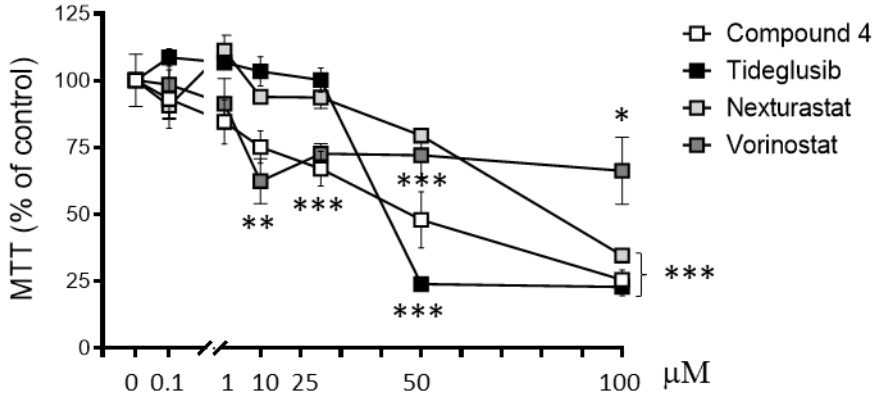

Figure SI7. SH-SY5Y cell viability was assessed through MTT assay after 24 h of treatment with: vehicle (0.1% DMSO) or increasing concentrations (0.1 µM, 1 µM, 10 µM, 25 µM, 50 µM, and 100 µM) of compound **4** (n = 10), tideglusib (n = 5), nexturastat A (n =5), or vorinostat (n = 5). The graph shows the dose-dependent effect of treatments as a percentage of the vehicle-treated condition (0 µM). Values are given as means ± SEM. *$p < 0.05$, **$p < 0.01$, ***$p < 0.001$. Turkey's test after two-way ANOVA.

9.

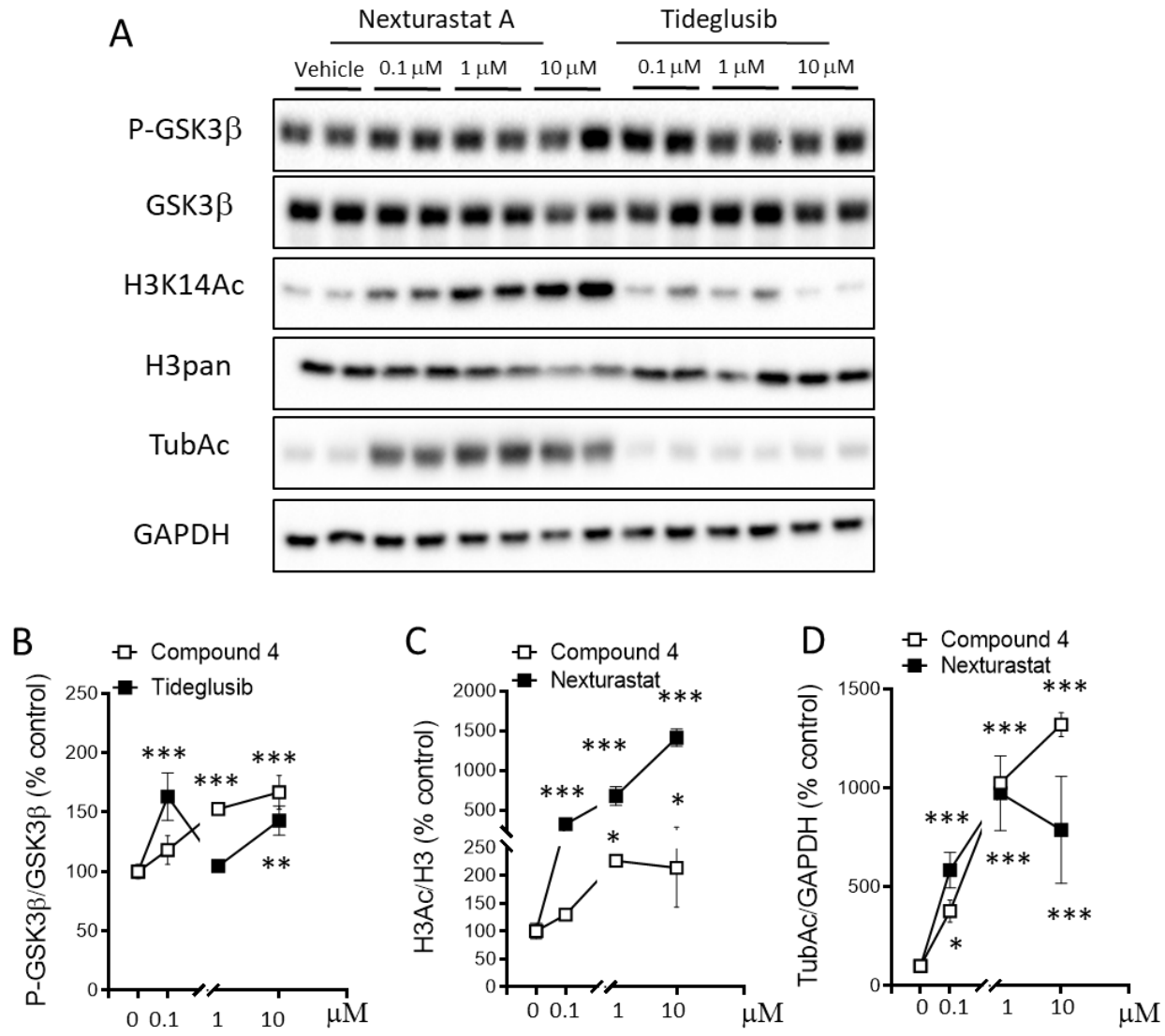

Figure SI8. A) Effect of treatment with Nexturastat A and Tideglusib on GSK-3β phosphorylation, histone H3 acetylation, and alpha tubulin acetylation in SH-SY5Y cells. Western blot analysis of phospho-GSK3β (Ser9; P-GSK-3β), acetylated H3 (H3Ac) and alpha tubulin (TubAc) levels in protein extracts from SH-SY5Y cells treated with vehicle (0.1% DMSO) or different concentrations (0.1 μM, 1 μM and 10 μM) Nexturastat A or Tideglusib for 24 h. Immunoblots are examples from two biological replicates of each experimental condition. B-D) Graphs show P-GSK-3β protein levels normalized to corresponding total protein levels (B), acetylated H3 levels normalized to total

H3 levels (C), and acetylated alpha tubulin (TubAc) levels normalized to GAPDH levels in cells treated as in A (C). Data in B-D are expressed as a percentage of vehicle-treated cells. Values are represented as means ± SEM. *p < 0.05, ** p < 0.01, *** p < 0.001. Fisher's LSD test after two-way ANOVA.

10.

a)

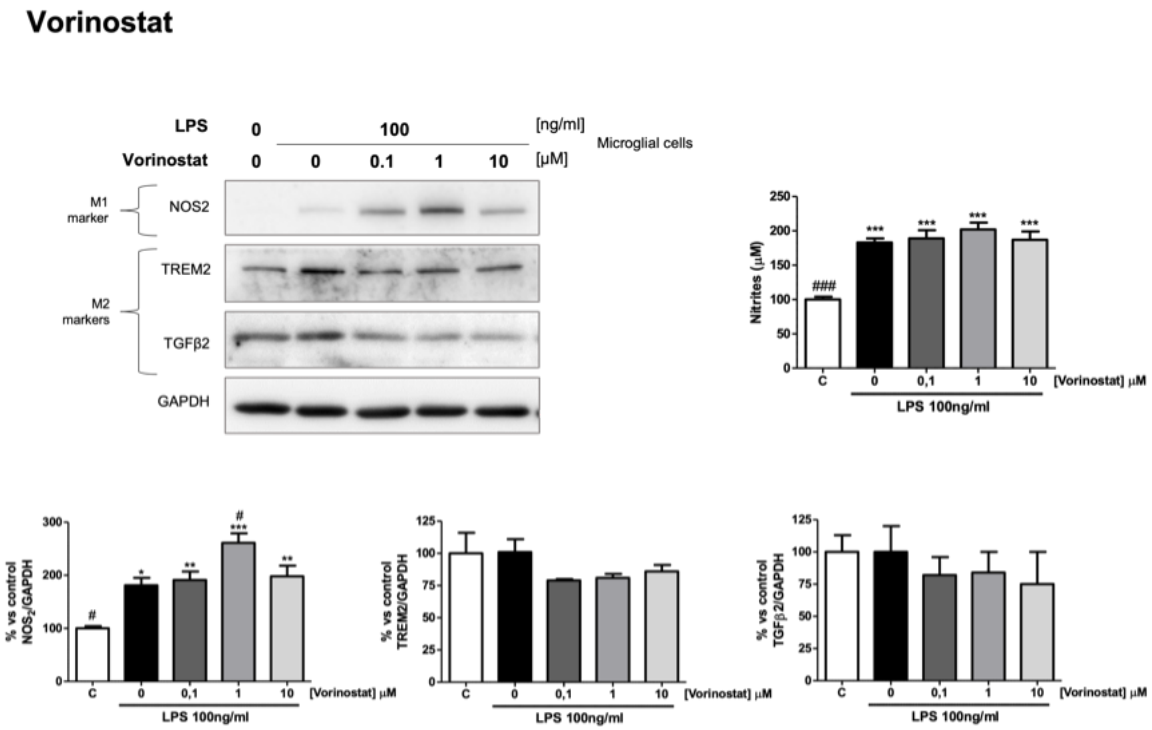

b)

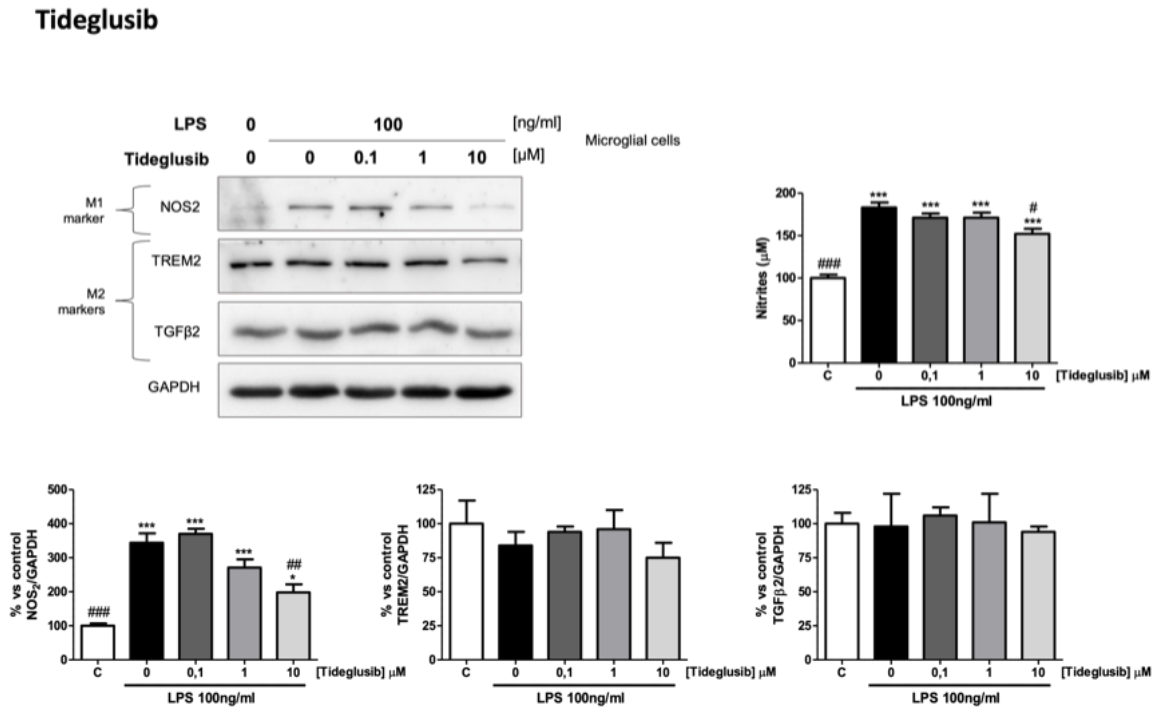

Figure SI9. Effect of a) Vorinostat, and b) Tideglusib on murine N9 cells following induction into M1 activation state by LPS (100 ng/mL) treatment. iNOS, TREM2, and TGFβ2 expression were analyzed using Western blot after a 24 h treatment with LPS and increasing concentrations (0.1, 1, and 10 μM). For the indirect determination of Nitric Oxide (NO) release, nitrites derived from N9-cultured media were quantified through Griess reaction. Results are presented as means ± SE from three independent experiments. Statistical significance was calculated using two-way ANOVA (Dunnett's post-hoc comparison test): # P <0.05, ## P <0.01, ### P <0.001, compared to LPS-activated microglia; * P <0.05, ** P <0.01, *** P <0.001, compared to control.

11.

Table SI2. Assessment of compound **4** and parent compounds tideglusib and vorinostat with respect to some Molecular-Structural and Physicochemical properties.

Properties[a]	compound **4**	Tideglusib	Vorinostat
MW	393	334	264
HB acceptors	4	2	3
HD donors	2	0	3
rotable bonds	5	3	10
cLogP[b]	3.33	5.21	0.99
Lipinski violation	No	No	no
PAINS	No	No	no
GI absorption	high	high	high
P-gp substrate	no	no	no

[a.] Obtained from http://www.swissadme.ch/, with the exception of [b.] that was obtained from ChemDraw 21.0.0.

12. Representative copies of ^{1}H-NMR and ^{13}C-NMR spectra.

Compound 2. ^{1}H-NMR (400 MHz) and ^{13}C-NMR (100 MHz) in DMSO-d.

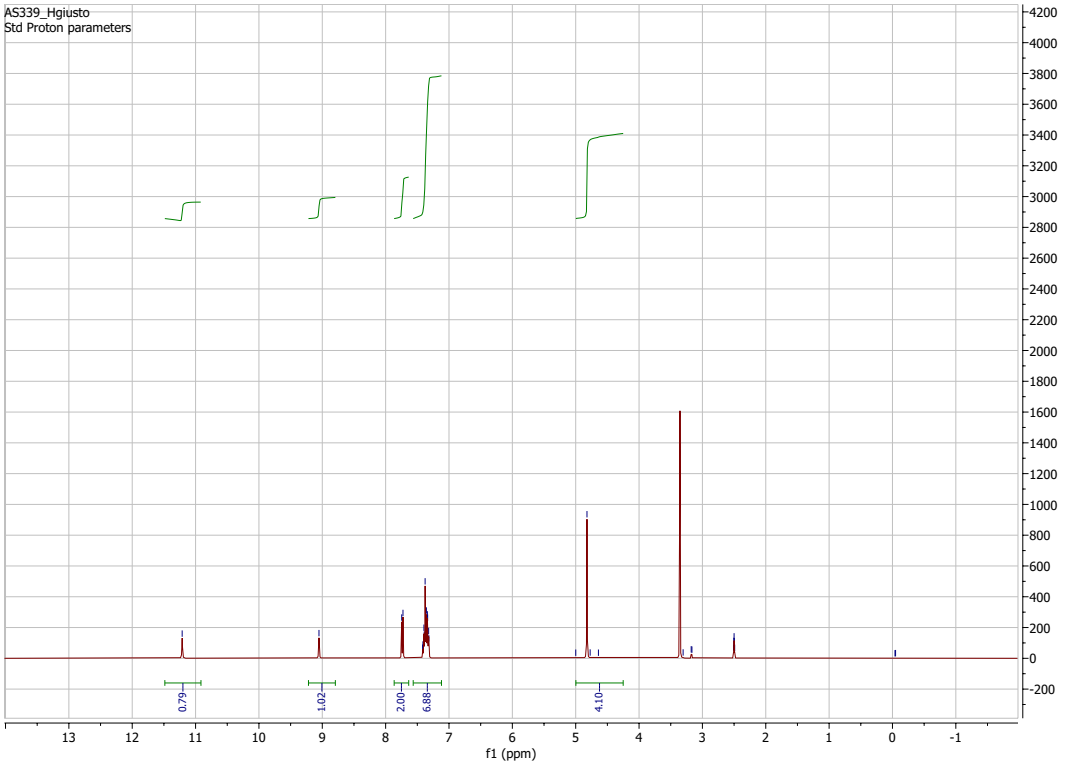

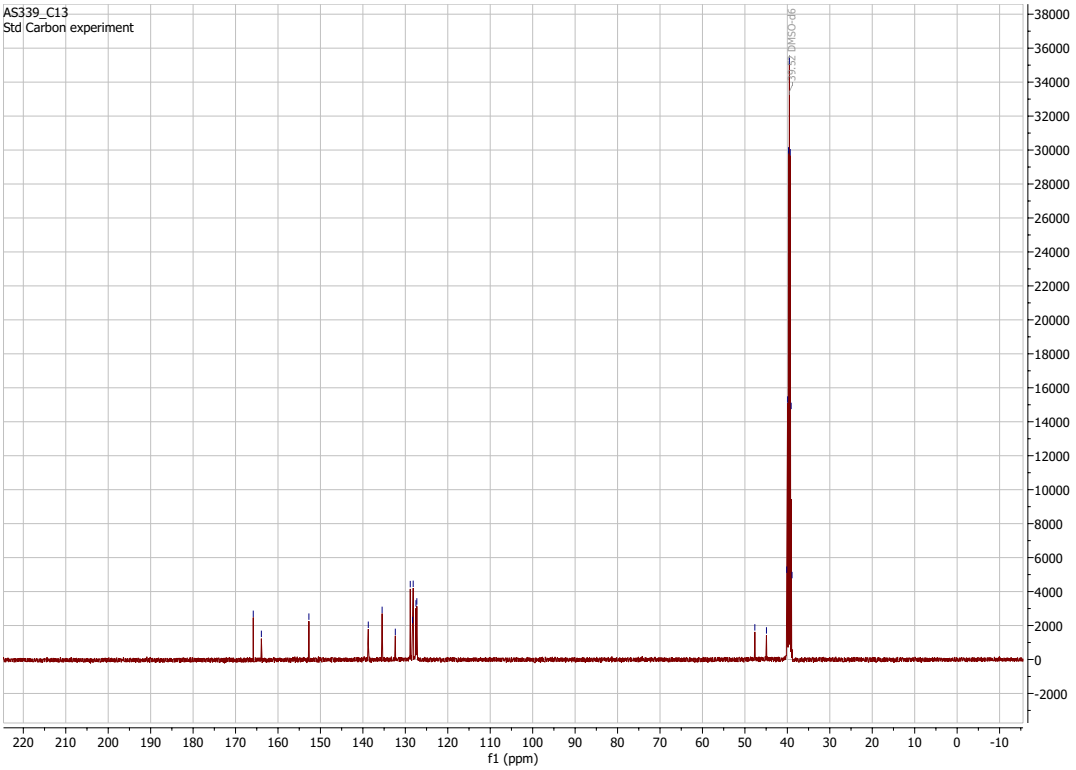

Compound 3. ^{1}H-NMR (400 MHz) and ^{13}C-NMR (100 MHz) in DMSO-d

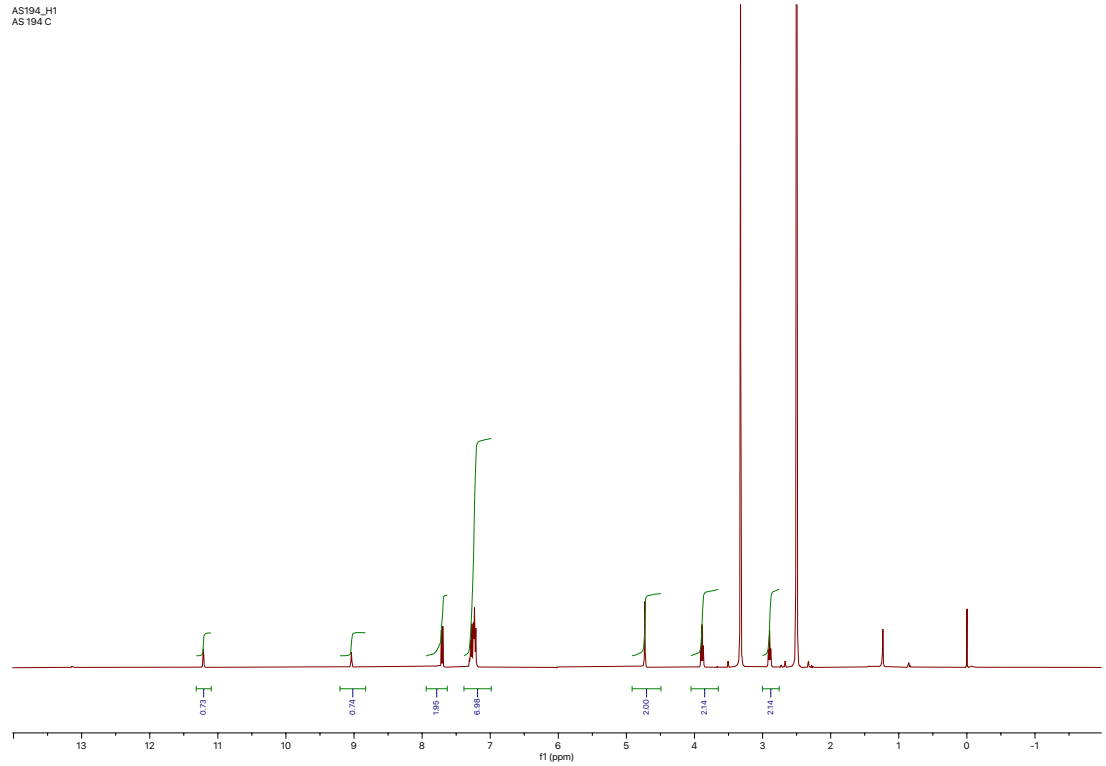

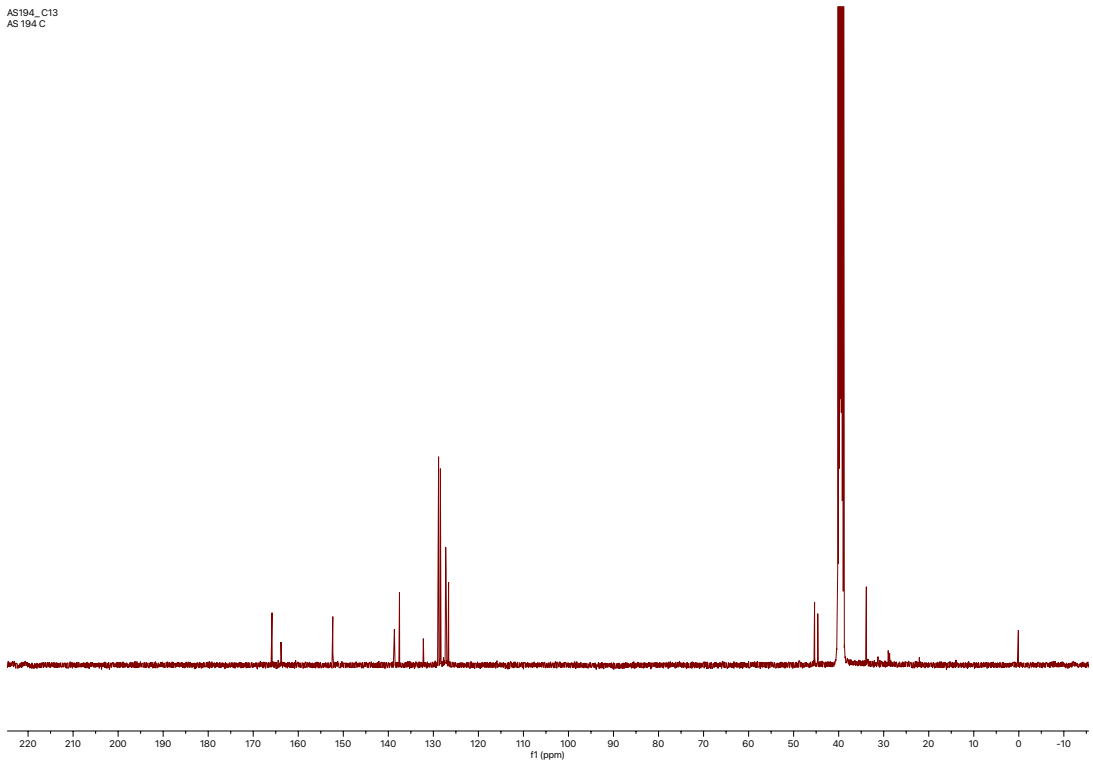

Compound 4. ^{1}H-NMR (400 MHz) and ^{13}C-NMR (100 MHz) in DMSO-d

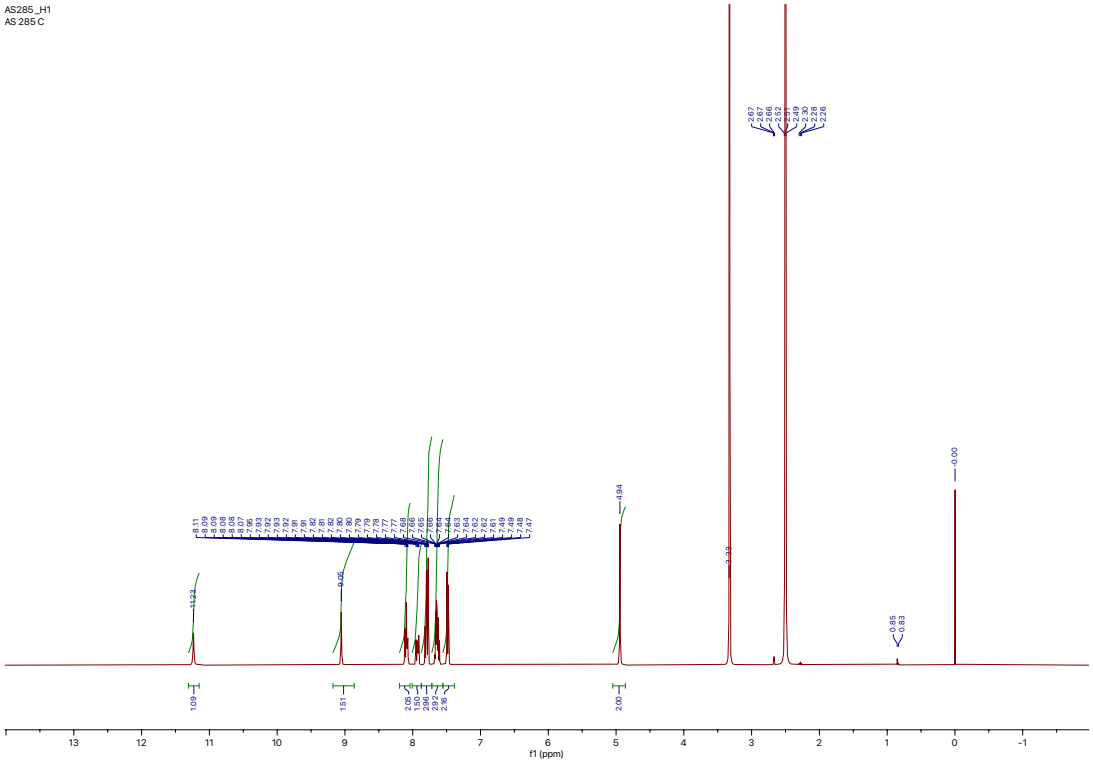

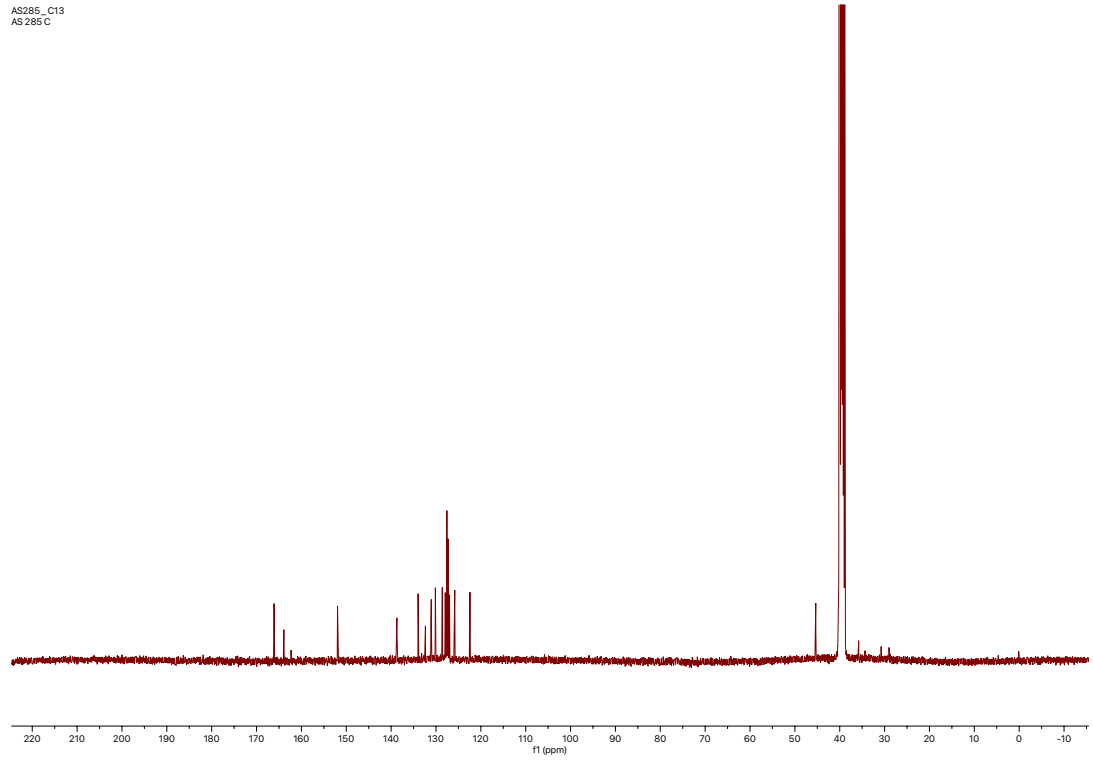

Compound 5. ^{1}H-NMR (400 MHz) and ^{13}C-NMR (100 MHz) in DMSO-d

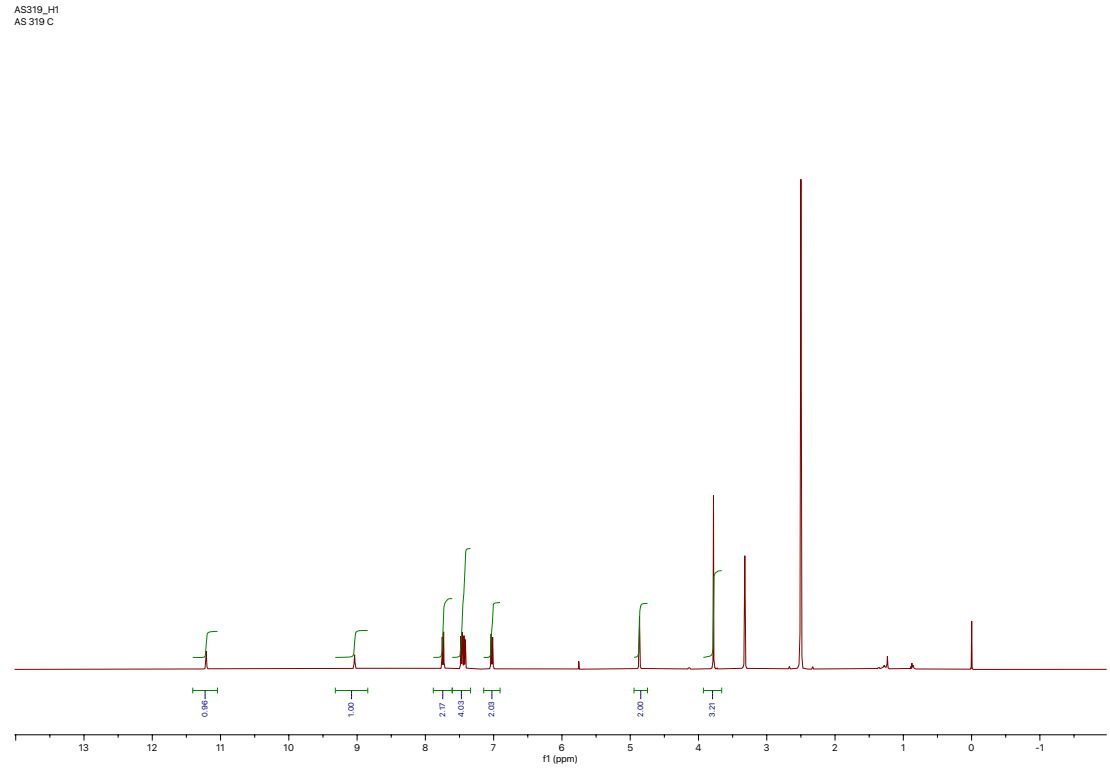

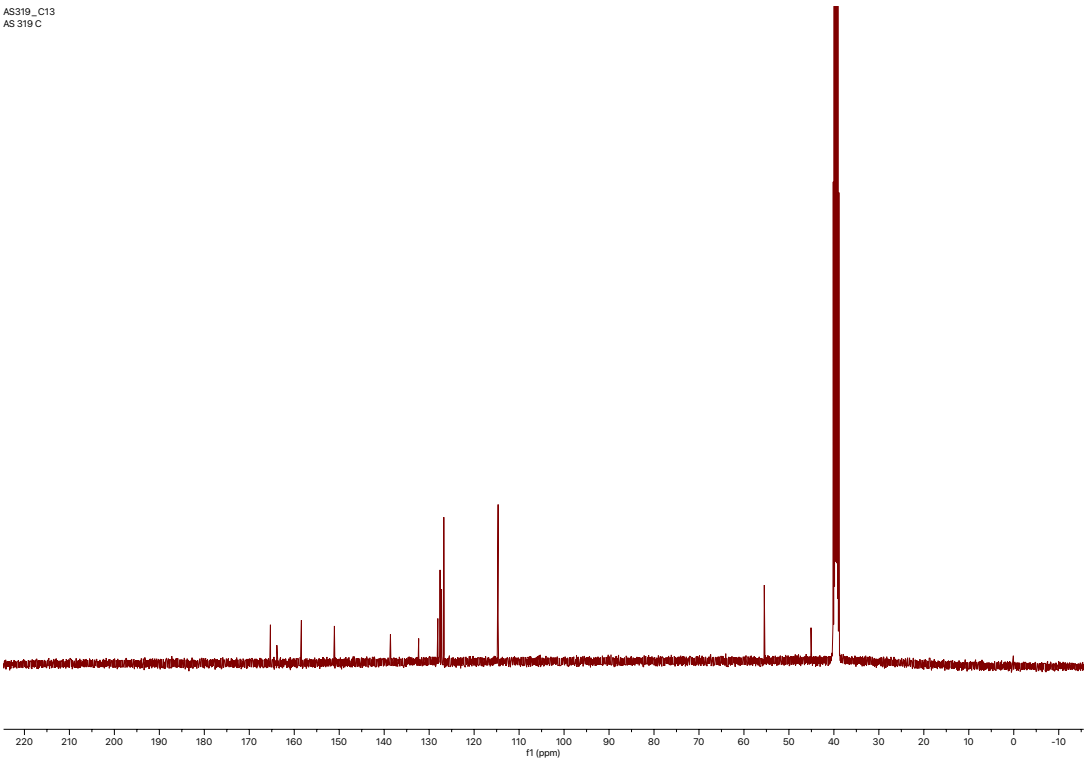

Compound 6. ^{1}H-NMR (400 MHz) and ^{13}C-NMR (100 MHz) in DMSO-d

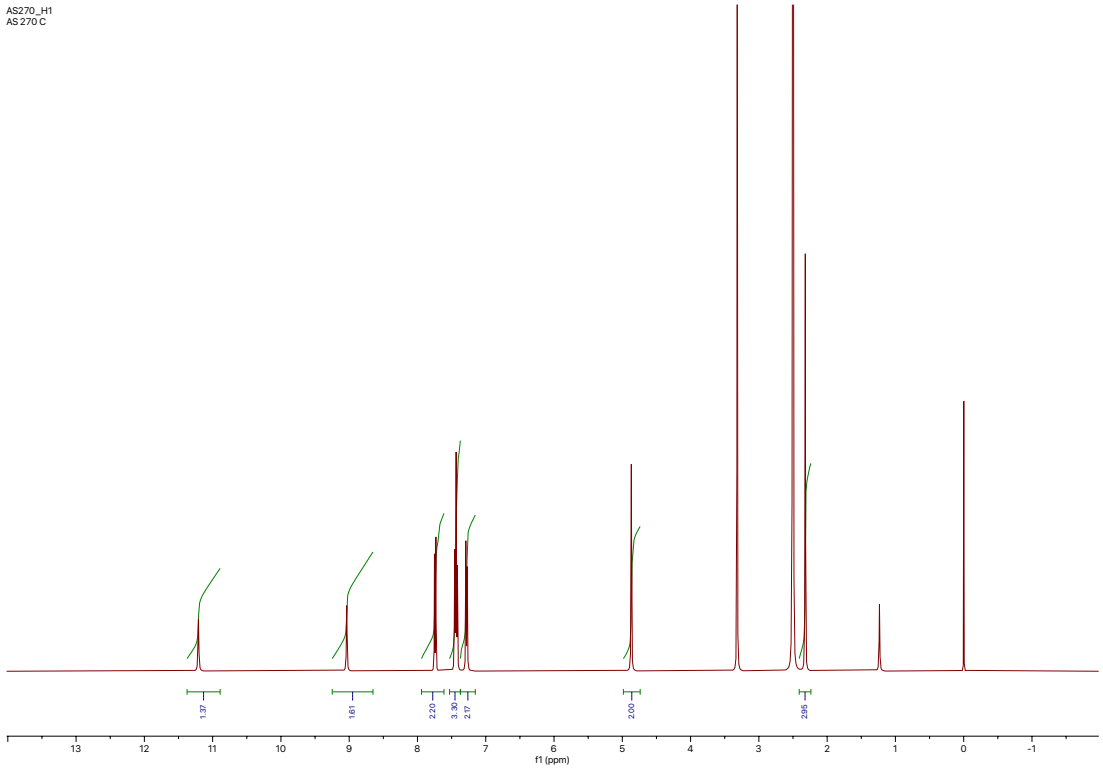

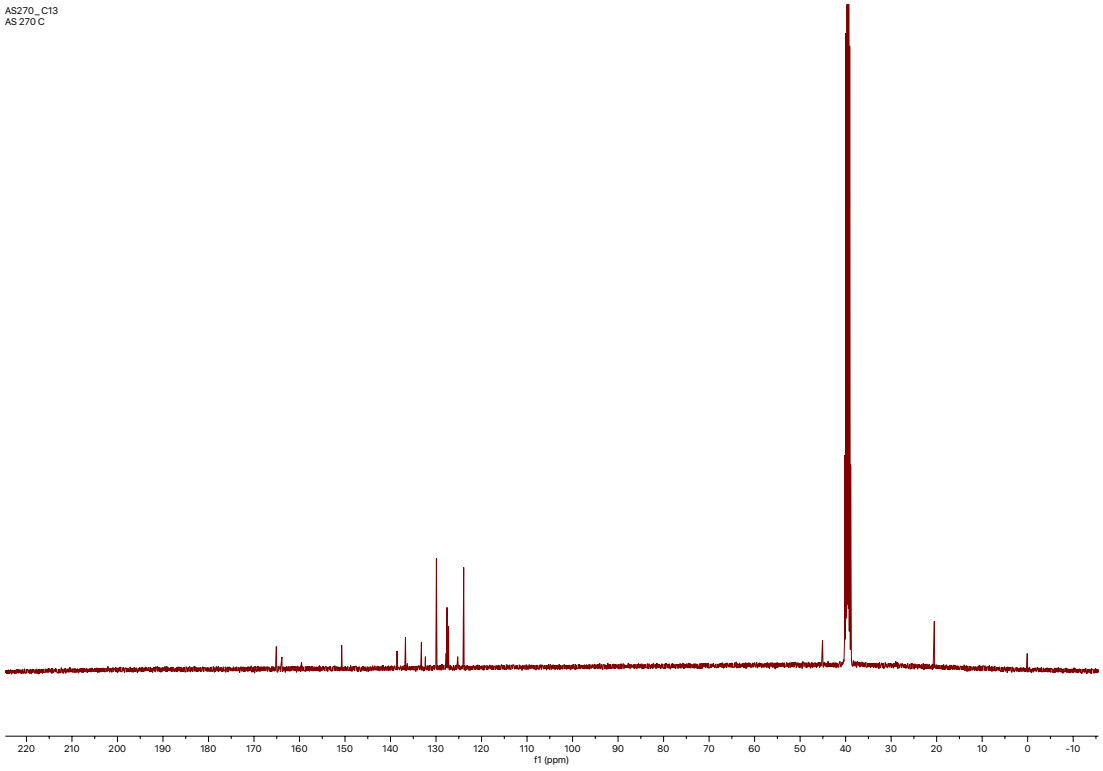

13.

Table SI3. List of antibodies used.

Antibody against	**Description**	**Diluition**	**Product nr and Manufacturer**
Phospho-GSK-3β (Ser9)	Rabbit polyclonal	1:1000	5558, Cell Signaling Technology
GSK-3β	Rabbit polyclonal	1:1000	9315, Cell Signaling Technology
Acetylated Tubulin	Mouse monoclonal	1:1000	T6793, Sigma-Aldrich
α-Tubulin	Mouse monoclonal	1:1000	T5168, Sigma-Aldrich
H3K9/14ac	Rabbit polyclonal	1:500	C15410005, Diagenode
Histone H3	Rabbit monoclonal	1:1000	05-928, Merck Millipore
GAPDH	Rabbit polyclonal	1:5000	G9545, Sigma-Aldrich
iNOS (D6B6S)	Rabbit polyclonal	1:1000	13120S, Cell Signalling Technology
TREM2	Rabbit monoclonal	1:1000	PA5-87933, Invitrogen, Thermo Fisher Scientific
TGFβ2	Mouse polyclonal	1:1000	Ab36495, Abcam
Secondary antibodies			
Antibody	**Conjugate**	**Diluition**	**Product nr and Manufacturer**
Goat Anti-Rabbit IgG	HRP	1:5000	111-035-144, Jackson ImmunoResearch Laboratories, Inc.
Goat Anti-Mouse IgG	HRP	1:5000	115-035-146, Jackson ImmunoResearch Laboratories, Inc.